Journal of Sciences, Islamic Republic of Iran 23(1): 45-58 (2012) http://jsciences.ut.ac.ir
University of Tehran, ISSN 1016-1104

Geochemical Aspects of Na-Metasomatism in Sargaz Granitic Intrusion (South of Kerman Province, Iran)

H. Ahmadipour[1,*] and G. Rostamizadeh[2]

[1]*Department of Geology. Faculty of Sciences, Shahid Bahonar University of Kerman, Kerman, Islamic Republic of Iran*
[2]*Departement of mining, Islamic Azad University, Kerman branch, Kerman, Islamic Republic of Iran*

Received: 12 June 2011 / Revised: 26 February 2012 / Accepted: 29 April 2012

Abstract

The Sargaz granitic intrusion has been emplaced in Sargaz ophiolitic suite, south-east of Sanandaj-Sirjan metamorphic zone, south of Kerman province. The central part of the intrusive body contains pinkish coarse-grained granite, but the fractured northern part, neighboring Chah-Mazraeh fault, has been subjected to pervasive Na-metasomatism and related subsolidus reactions. In the northern altered rocks, the primary magmatic textures have been changed into a new generation of albite along with chlorite, epidote and sericite. Petrographically, in Sargaz altered rocks, albite occurs as overgrowth, crack-filling, vug-filling and interstitial forms. The first form has been replaced the primary plagioclase, and/or alkali feldspars by a coupled dissolution-reprecipitation mechanism, while, the other forms have been crystallized from Na-rich alkali fluids during Na-metasomatism. In Sargaz unaltered granites, primary feldspars contain oligoclase ($An_{23.8}$-$An_{10.6}$) and K-feldspar (kf_{70}-$kf_{95.9}$), while, metasomatic feldspars are entirely albite ($An_{8.4}$-$An_{0.3}$) without any chemical zonation. Na-metasomatism in these rocks resulted obvious mass changes in rock composition, as the altered rock are enriched in Na, La, Y, Yb, Hf and Th and depleted in K, Fe, Mg, Ca, Sr, Co and Zn. Si, P, Rb, Ti, Al and Zr possibly acted as immobile elements during Na-metasomatism. Evidences in Sargaz intrusion show that alkali Na-rich fluids caused Na-metasomatism as dissolution of primary quartz and then, crystallization of albite. Microcracks facilitated infiltration of fluids. During the metasomatism, enough quartz grains were dissolved, thereby releasing silica for the formation of different forms of new albites, thus, the role of quartz dissolution, is more important than those expected earlier.

Keywords: Sargaz granitic intrusion; Na-metasomatism; Albitization; Dissolution-reprecipitation

Introduction

Na-metasomatism represents the circulation of Na-rich fluids and widespread changes in several types of lithologies such as deuterically altered granitic rocks, alkali carbonatite complexes, volcanic and sedimentary rocks and also in metamorphic environments associated with regional scale ductile shear zones ([38,43]).

* Corresponding author, Tel.: +98(913)3430397, Fax: +98(341)3222035, E-mail: hahmadi@mail.uk.ac.ir

Archive of SID

www.SID.ir

Furthermore, Na-metasomatism in granitic rocks develops either during hydrothermal activity [28] or occurs after emplacement and cooling of intrusion ([11,41,44,40]). This type of metasomatism produces various distinct features such as myrmekite formation [12,13], dissolution of quartz [11], crystallization of different shapes of new albites [8,10,40] and various chemical changes in the whole rock chemistry [33,39].

In the Sargaz granitic intrusion, the granitic rocks have been subjected to pervasive post magmatic Na-metasomatic process. Northern parts of Sargaz intrusion are characterized by metasomatism of primary feldspars, biotites and amphiboles and dissolution of quartz grains. The mineralogical assemblage of these rocks is similar to some hydrothermal parageneses related to post magmatic events ([25,22,2]) and records all evidences implying Na-metasomatism of the Sargaz granite. In order to clarify the nature of Na-metasomatism and the physico-chemical conditions of overgrowth albite, petrography, mineral and whole rock chemical analyses of Sargaz granitic samples have been carried out. The aim of this study is showing Na-metasomatism and its chemical and petrographical aspects in Sargaz granite in order to understanding of gold mineralization (and other precious metals) in such environments. There are several intrusions in the world in which gold mineralization [14,23] and uranium deposition [30] associate with Na-metasomatism, so it is important to investigate the effects of this metaso-matism in the Iranian granitic intrusions as a basis for the next exploration studies.

Material and Methods

Analytical Methods

In the present work, we need both altered and unaltered rock samples for comparison and for chemical analyses, so altered samples collected carefully from outcrops in the northern fracture zones, while, unaltered samples took from the least altered central parts of Sargaz intrusion. Petrographical features of Na-metasomatism were studied in thin sections and then, for mineralogical studied, mineral chemical analyses were obtained by a GEOL JXA, 8900 superprobe in the Münster University microprobe laboratory (Germany) using an accelerating voltage of 15 kv, probe current of 5µA and beam diameter of 5µm. Counting time for each analysis was 15 s. Chemical composition of whole rocks have been performed by (ICP-AES) (major elements) and ICP-MS (minor elements) in the laboratory of ALSCHEMEX in Canada.

Geological Setting and Field Characteristics of Sargaz Iintrusion

General geological characteristics of the Sagaz granitic intrusion have been stated in the geological map of Sabzevaran [4] as the only published work that has been done on this intrusion. As indicated in this map, the Sargaz granite crops out over an area of 7.5 km^2 and has been emplaced into the Sargaz ophoiolitic suite, 40 km west of Jiroft town, Kerman province, Iran. Sargaz ophiolitic suite of Jurassic in age, [4] is located at the south-eastern Sanandaj-Sirjan metamorphic zone and comprises of propylitized pillow lavas, radiolarian chert, tuff, hyaloclastites and flysch type sedimentary rocks. The suite has been cut by several granitic intrusions (e.g. Sargaz granite) and numerous diabasic dykes (Fig. 1). As shown in Figure 1 and Figure 2a, between the northern part of Sargaz intrusion and surrounding rocks, there is an altered, red-stained zone that marks the effects of Chah-Mazraeh fault movements and intense alteration on the granite and host rocks. A lot of fractured and faulted zones have been formed in the northern part due to movements of this fault. The Sargaz granite probably emplaced during upper Jurassic [4] in Sargaz ophiolitic suite and contains two parts; (1) unaltered alkali-feldspar leucocratic granite that appears as a coarse-grained reddish-pink colored outcrop with porphyritic texture in its margins. (2) Na-metasomatized granites occurring at the northern part of the pluton in the vicinity of Chah-Mazraeh fault. This part appears as coarse-grained grey colored rocks with Na-metasomatic alteration. In the field, large quartz grains (up to 10 mm in diameter), white colored feldspars and sparse altered ferromagnesian minerals can be seen. Within the northern part, several localized shear zones of brittle nature occur that are marked by intense epidotization (Fig. 2b). There are pinkish fine-grained aplitic veins (up to 30 cm in thickness) (Fig. 2c) and diabasic dykes in Sargaz intrusion.

Zones of Na-metasomatozed rocks are mainly related to fracture zones of northern part. The orientation of these zones are not defined, but they follow the strike of Chah-Mazraeh fault (East-West). The contact between unaltered and altered granites is gradational and in the field, this change can be traced by changing in color from pink to grey. The character of metasomatic alteration in Sargaz intrusion depends on structural factor. In other word, hydrothermal solutions could have been moved along the fractures and the flow became focused in fractured zones. Chah-Mazraeh fault may be the effective factor responsible for the fracturing of northern part of the Sargaz intrusion.

Archive of SID

www.SID.ir

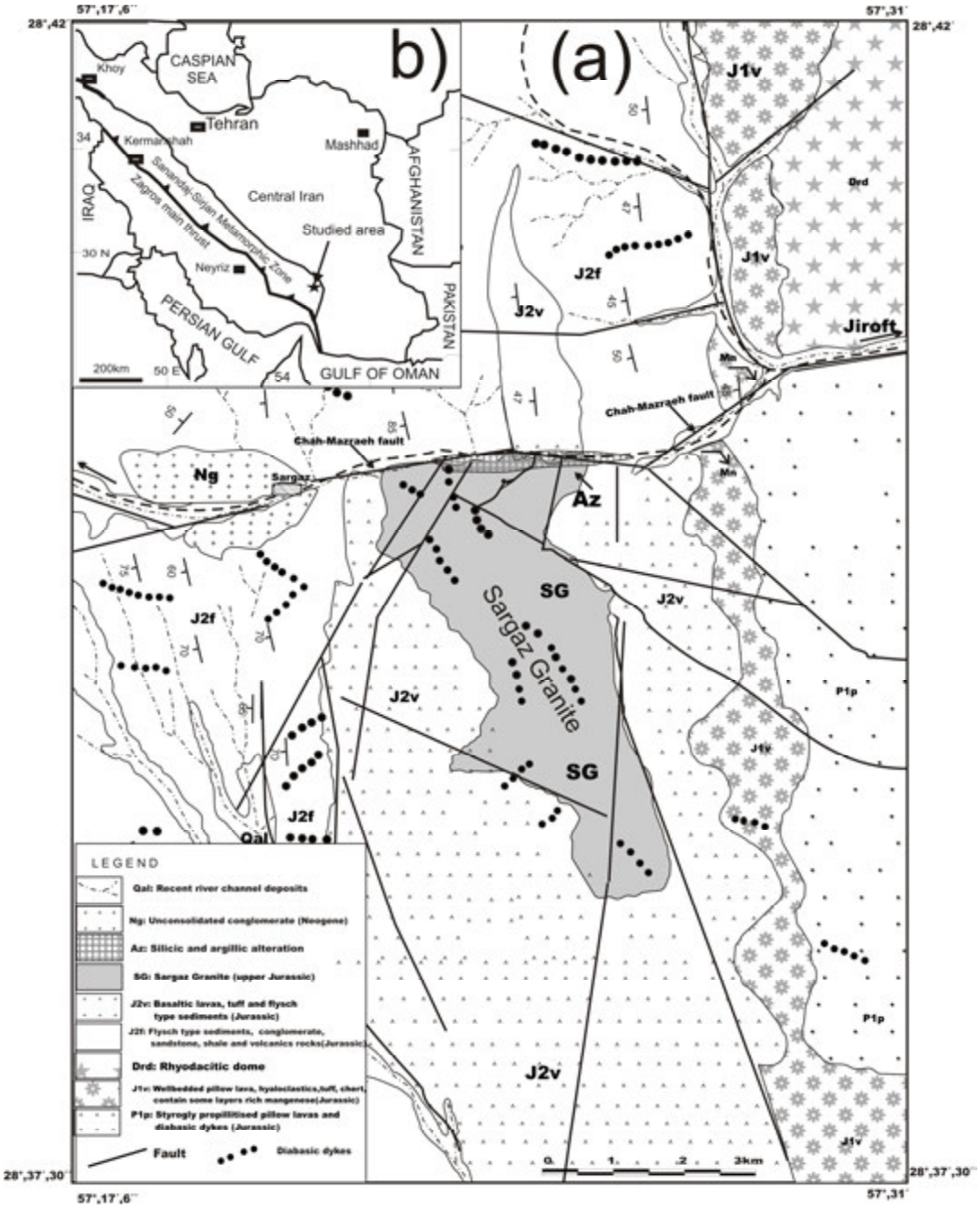

Figure 1. Geological map of Sargaz area (a), (modified after Babakhani et al., [4]) and location of this area in Iran (b).

Petrography

Sargaz intrusion is a leucogranite that in the northern part, has been changed into Na-metasomatic altered rocks with distinct petrographical characteristics. The least altered Sargaz granite is a leucocratic medium-to coarse grained and inequigranular rock. The main

www.SID.ir

mineral assemblage is quartz, plagioclase and biotite, with k-feldspar, hornblende, epidote, apatite and opaque minerals as accessory phases. Plagioclase is found as medium-sized (up to 2 mm in length) twinned euhedral to subhedral crystals that constitutes 40-45 vol%. It ranges from oligoclase to albite and sometimes shows compositional zoning. In unaltered Sargaz granites, quartz is found as large unhedral interstitial grains (up to 10 mm in diameter), constitute up to 40 vol% and may present undulatory extinction. Cracks are common in some of quartz grains but not in the adjacent feldspars. K-feldspar constitutes up to 7 vol% of these rocks and occurs as subhedral to unhedral perthitic crystals (up to 4mm in diameter), sometimes lying between plagioclase and quartz grains. In some samples, k-feldspar shows intergrowth texture as granophyre with average sizes ranging from 2-4 mm that generally clouded by fine sericites. Biotite is the main phase of the mafic minerals (up to 6 vol%), which has slightly chloritized at the margins and occurs as subhedral plates up to 1 mm long. The texture in the margin of Sargaz intrusion tends to be porphyritic with medium-grained quartz and feldspar phenocrysts embeded in a fine-grained randomly oriented quartz and feldspar groundmass.

Na-metasomatized granites in Sargaz intrusion are characterized by textures indicating subsolidus reactions. In these altered rocks, the most characteristic feature of Na-metasomatism is crystallization of new albites, but, partial sericitization of plagioclase, chloritization of biotite, epidotization of amphiboles, silicification and myrmekite shapes of quartz-plagioclase intergrowth are common. The general shapes of the magmatic feldspars has been preserved, but original granitic texture has partially obliterated. The former plagioclases (with oligoclase composition) have surrounded by an albitic rim (Fig. 3a) (with up to 0.5 mm in thickness) and biotite has been completely replaced by chlorite and opaque minerals. Quartz vugs have subsequently filled by the new albites during Na-metasomatism (Fig. 3b). In these albitized granites, Na-metasomatism leads to crystallization of unhedral, twinned albites (Fig. 3c). The contacts between new albites and older feldspars and quartz grains have irregular and concave form indicating dissolution of preexisting phases (Fig. 3c). In many cases, magmatic quartz grains have been fragmented and interstitial albite has been formed between quartz grains as a cement (Fig. 3d).

Texturally, there are four shapes of new albites in Sargaz altered granites; (1) overgrowth albite that is found around the former plagioclases (Fig. 3e), and sometimes appears as chessboard albite (Fig. 3a); (2) crack-filling albite that have been crystallized in the microcracks of quartz grains (Fig. 3f); (3) vug-filling albite that has filled the vugs of quartz (Fig. 3g), and (4) interstitial albites that formed between primary phases as a cement (Fig. 3f). These new albites totally, constitute up to 25 vol% of the altered granites.

Propylitic fault controlled alteration zones mainly occur as fissural related altered biotite and hornblende crystals. This alteration characterized by epidote + clinozoisite + chlorite + sericite assemblage. The close association between new albites and propylitic related

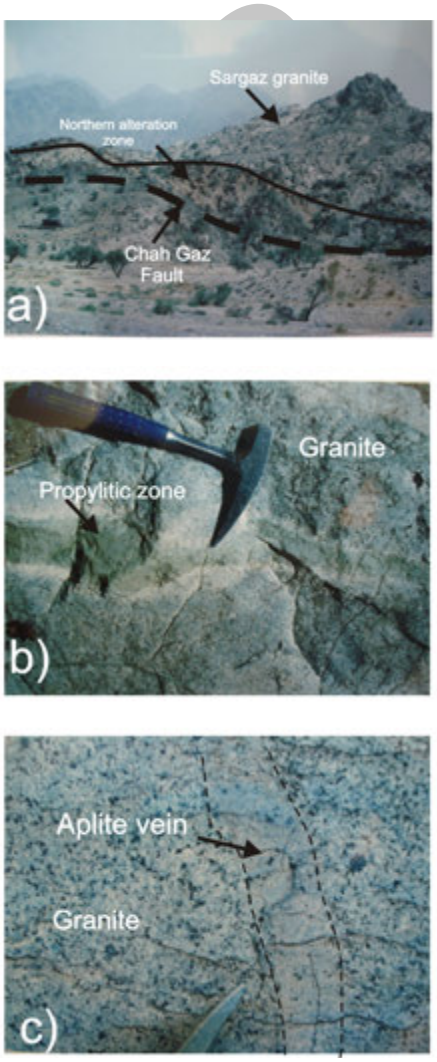

Figure 2. Field characteristics of Sargaz intrusion. a) Northern alteration zone between Sargaz granite and Chah Mazraeh fault; b) Propylitized zone in altered Sargaz granite that has filled by epidote; c) Fine-grained aplitic vein in Sargaz granite.

www.SID.ir

assemblage indicates that probably they formed during a single event. Sericitic alteration has affected the Sargaz granite in the final stages of alteration history and produced a lot of small sericite crystals distributed throughout the rocks. Silicification probably was the last stage that has imposed on the Sargaz granite (Fig. 4). In this stage, quartz veinlets have been formed (With up to 1 mm in thickness) and cut all of the previous phases as a network, without certain pattern, suggesting that they crystallized after Na-metasomatism of Sargaz intrusion.

Feldspar Chemistry

Table 1 shows representative analyses of different types of feldspars in Sargaz intrusion. In this Table, feldspars are divided into magmatic (primary) and metasomatic (secondary) groups. Those of magmatic occur in the least altered granites and contain plagioclases and k-feldspars, while metasomatic ones belong to the altered Sargaz granites and comprise overgrowth, crack-filling, vug-filling and interstitial albites. Chemical compositions of magmatic plagioclases change from oligoclase to albite ($An_{10.55}$-$An_{23.83}$) and magmatic k-feldspars show distinctive compositions ($kfs_{74.5}$- $kfs_{95.9}$). Metasomatic feldspars have albitic compositions ($An_{1.04}$-$An_{7.81}$), as shown in Figure 5 and Table 1. In analyzed samples, these shapes of albites show similar chemical compositions without any significant chemical zonation.

Whole Rock Chemistry

Chemical compositions of Sargaz granites are presented in Table 2. In different geotectonic diagrams, Sargaz granitic samples plot into a restricted area due to their homogenous compositions. The samples are transitional between calc-alkaline and sub-alkaline (Fig. 6a), while, the A/NK versus A/CNK diagram clearly illustrates the peraluminous nature of all samples (Fig. 6b). In the Y versus Nb diagram, the samples tend to volcanic arc field, some of them plot from the boundary line, toward the within plate granite field (Fig. 6c). Sargaz granites show a weak LREE-enrichment REE patterns with distinct Eu anomaly and the REE patterns for the least altered and altered samples are almost similar (Fig. 7), suggesting that REE contents are not correlated with the intensity of Na-metasomatism and it may be a primary feature of magmatic evolution. Association of Sargaz granite intrusion with pillow lavas of Sargaz ophiolite and the contents of K2O, Ba, Rb, Cr, Sr show that this intrusion is very similar to M-type granites.

Results and Discussion

Evidences for Na-Metasomatism

The mineral assemblage of Sargaz intrusion with development of albite, chlorite and epidote in altered parts, suggest a possible alteration and/or hydrothermal event. Field and petrographic studies revealed that this event has been controlled by Chah-Mazraeh fault related fracturing and dissolution of quartz.

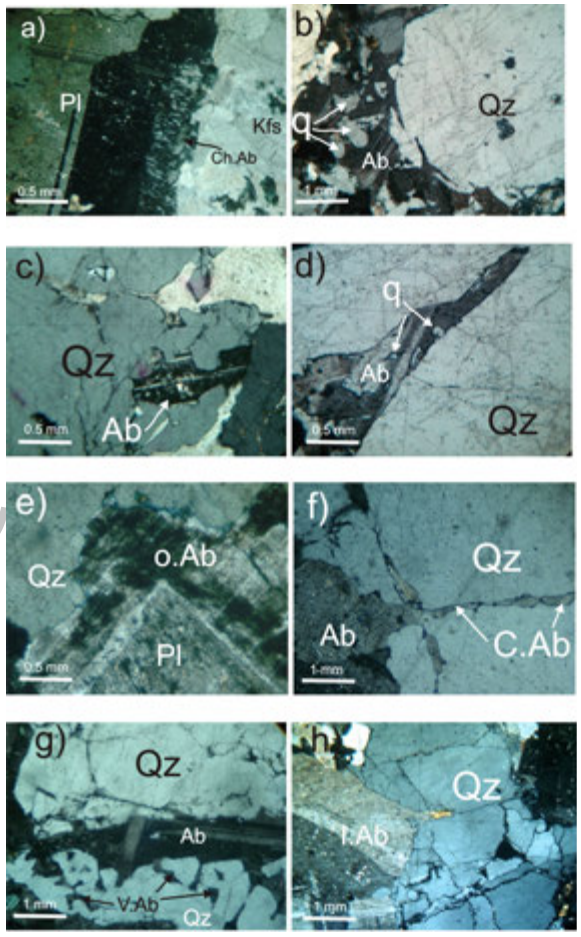

Figure 3. Textural features of Sargaz granite; a) Chessboard albite (ch.Ab) in contact with magmatic plagioclase (Pl) and K-feldspar (Kfs); b) Quartz fragments (q) among new albite (Ab) and dissolution of magmatic quartz (Qz), note the irregular grain boundary between the Qz and Ab; c) Formation of new twinned albite (Ab) in the pores of quartz grains; d) crystallization of new albite (Ab) in the fractures of quartz grain. New albite surrounded by quartz fragments (q); e) Overgrowth albite (O.Ab) which has been formed between magmatic plagioclase and quartz; f) Crack-filling albite (C.Ab) in microcracks of quartz grain; g) Vug-filling (V.Ab) and interstitial (I.Ab) albites; h) interstitial albite (I.Ab).

Archive

www.SID.ir

Table 1. Representative feldspars compositions from Sargaz granite

Rock Type	**Least Altered Sargaz Granite**						**Altered Sargaz Granite**							
Mineral	Magmatic plagioclases			Magmatic K-feldspars			Overgrowth Albite		Crack-filling Albite		Vug-filling Albite		Interstitial Albite	
Sample	*S86*	*S86*	*S5*	*S86*	*S5*	*S5*	*S85*	*S44*	*S85*	*S85*	*S33*	*S33*	*S85*	*S33*
Wt%														
SiO2	65.89	64.01	62.67	66.08	66.08	65.96	67	68.06	69.43	69.2	69.38	70.01	69.89	70.01
TiO2	0	0	0	0.04	0	0	0	0	0	0	0	0	0	0
Al2O3	21.01	22.45	23.54	17.98	18	17.14	19.5	19.56	19.54	18.98	19.75	19.52	19.37	20.03
Fe2O3	0.16	0.5	0.1	0.08	0	0.17	0	0.08	0.02	0	0.15	0	0	0
CaO	2.3	3.4	4.89	0.07	0.02	0.23	1.54	0.3	0.22	0.02	0.3	0.3	0.09	0.1
Na2O	10.68	9.64	8.54	2.79	0.44	0.5	9.98	11.59	11.47	11.84	11	10.28	11.35	11.2
K2O	0.15	0.14	0.15	12.54	16.14	16.58	0.1	0.3	0.16	0.03	0.07	0.23	0.1	0.11
Total	100.19	100.14	99.89	99.58	100.68	100.58	98.12	99.89	100.84	100.07	100.65	100.34	100.8	101.45
Number of ions on the basis of 32 oxygene														
Si	11.56	11.33	11.15	12.15	12.15	12.16	12.06	11.91	12.06	12.08	12.13	12.33	12.16	12.11
Ti	0.00	0.00	0.00	0.01	0.00	0.00	0.00	0.00	0.00	0.00	0.00	0.00	0.00	0.00
Al	4.34	4.68	4.94	3.90	3.90	3.72	4.14	4.03	4.00	3.90	4.07	4.05	3.97	4.08
Fe	0.00	0.00	0.00	0.00	0.00	0.00	0.00	0.00	0.00	0.00	0.00	0.00	0.00	0.00
Ca	0.43	0.64	0.93	0.01	0.00	0.05	0.30	0.06	0.04	0.00	0.06	0.06	0.02	0.02
Na	3.63	3.31	2.95	0.99	0.16	0.18	3.48	3.93	3.86	4.01	3.73	3.51	3.83	3.76
K	0.03	0.03	0.03	2.94	3.79	3.90	0.02	0.07	0.04	0.01	0.02	0.05	0.02	0.02
mol%														
Ab	88.633	83.024	75.302	25.181	3.974	4.334	91.586	96.962	98.061	99.741	98.111	97.007	98.992	98.873
An	10.548	16.182	23.828	0.349	0.100	1.102	7.810	1.387	1.039	0.093	1.479	1.564	0.434	0.488
Kfs	0.819	0.793	0.870	74.470	95.926	94.564	0.604	1.651	0.900	0.166	0.411	1.428	0.574	0.639

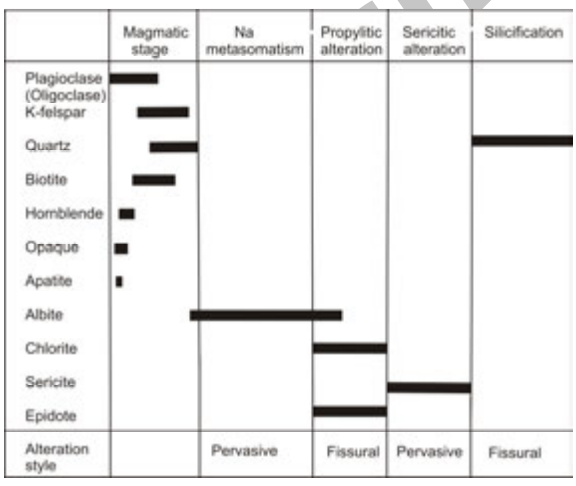

Figure 4. Magmatic, Na-metasomatic, propylitic, sericitic and silicification crystallization sequences in the Sargaz granite.

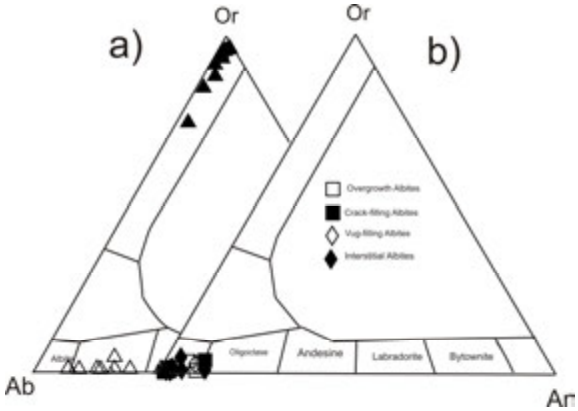

Figure 5. Or-Ab-An diagrams showing the composition of magmatic (a) and metasomatic (b) feldspars from Sargaz granite.

Archive of SID

www.SID.ir

Table 2. Whole rock chemical data for Sargaz granite

Rock type	**Least altered granites**		**Altered granites**					
Sample	*SA31*	*SA32*	*SA2*	*SA4*	*SA7*	*SA8*	*SA11*	*SA12*
SiO2	72.87	73.09	73.19	73.01	73.41	73.21	75.98	73.41
TiO2	0.26	0.27	0.29	0.24	0.25	0.23	0.15	0.26
Al2O3	12.00	12.51	12.49	12.31	12.68	13.75	12.81	12.84
Fe2O3t	3.75	3.14	3.10	3.51	3.51	3.14	1.46	2.51
MnO	0.06	0.09	0.04	0.12	0.12	0.06	0.01	0.06
MgO	0.78	0.81	0.85	0.79	0.64	0.74	0.21	0.58
CaO	2.57	2.50	1.24	1.12	1.14	1.19	0.88	0.87
Na2O	4.89	4.78	6.30	5.57	6.12	6.10	6.71	6.11
K2O	2.50	1.46	1.17	1.21	0.34	0.35	0.58	0.31
P2O5	0.04	0.04	0.05	0.06	0.04	0.05	0.03	0.04
LOI	0.88	0.98	0.96	1.63	0.78	1.02	0.73	2.35
Total	100.60	99.67	99.68	99.57	99.03	99.84	99.55	99.34
Traces ppm								
Ba	169	174	168	110	179	106	185	165
Co	8	6	6	8	8	6	2	5
Cr	135	163	179	164	187	149	200	162
Cs	1.5	2.1	5.6	9.3	7.8	4.0	5.3	5.5
Ga	26.1	27.4	20.9	20.3	21.0	21.2	24.1	21.5
Hf	5.5	4.9	9.6	3.5	8.2	9.1	12.1	8.0
Nb	13.2	18.1	24.4	18.7	20.0	20.0	41.1	23.4
Ni	14	13	18	15	19	17	20	17
Rb	17	16	17	19	20	21	19	19
Sr	198	214	141	154	131	159	118	110
Ta	2.6	2.7	3.1	3.0	3.2	3.3	4.8	3.7
Th	21.4	28.0	36.5	40.3	36.8	40.3	40.3	40.3
V	24.0	21.0	23.1	20.5	20.4	22.4	7.4	16.7
Y	18.7	21.8	29.5	19.2	16.8	237.0	53.1	24.2
Zn	36	37	32	31	30	35	26	32
Zr	184	142	198	126	174	169	332	171
La	47.5	69.8	45.6	71.4	72.1	50.5	55.2	69.2
Ce	96.4	124.0	92.1	119.0	123.0	95.2	99.2	119.0
Pr	10.8	14.8	9.7	15.5	15.4	12.6	13.5	15.4
Nd	42.8	58.5	39.9	58.2	61.2	44.2	55.4	56.3
Sm	7.8	9.8	8.1	11.4	12.0	10.3	9.6	11.2
Eu	0.8	0.9	0.7	1.4	1.2	0.8	0.9	1.2
Gd	6.8	7.5	6.1	8.5	8.7	7.5	7.8	7.9
Tb	1.0	1.2	1.0	1.4	1.4	1.1	0.9	0.9
Dy	6.9	7.2	6.9	7.4	7.5	7.9	6.5	6.8
Ho	1.4	1.4	1.4	1.5	1.5	1.6	1.3	1.1
Er	4.5	4.4	4.6	4.5	4.8	5.1	5.1	6.1
Tm	0.8	0.7	0.7	0.8	0.8	0.9	0.9	1.0
Yb	4.2	4.0	3.9	4.0	4.2	5.1	4.5	4.1
Lu	0.6	0.5	0.5	0.7	0.6	0.7	0.6	0.8

Archive of SID

www.SID.ir

Table 2. (continued)

Rock type	**Altered granites**								
Sample	*SA15*	*SA16*	*SA17*	*SA20*	*SA21*	*SA22*	*SA23*	*SA28*	*SA30*
SiO2	74.69	73.80	73.10	71.02	70.28	73.49	76.10	74.11	76.64
TiO2	0.22	0.31	0.27	0.37	0.44	0.24	0.22	0.19	0.27
Al2O3	12.66	12.59	13.45	12.49	13.12	12.41	13.68	13.14	12.54
Fe2O3t	2.24	3.05	3.31	4.30	5.18	3.06	1.43	2.24	2.80
MnO	0.03	0.05	0.04	0.05	0.07	0.04	0.01	0.01	0.05
MgO	0.44	1.06	0.71	1.87	1.50	0.47	0.27	0.54	0.61
CaO	0.73	1.01	1.48	1.41	1.05	1.86	0.59	0.99	1.21
Na2O	5.61	6.13	6.14	5.61	5.81	4.71	6.74	6.78	4.79
K2O	1.56	0.28	0.24	0.54	1.24	1.32	0.13	0.16	1.34
P2O5	0.03	0.06	0.05	0.07	0.13	0.05	0.07	0.04	0.03
LOI	0.91	1.32	1.20	1.89	0.56	1.93	1.00	1.53	0.86
Total	99.12	99.66	99.99	99.62	99.38	99.58	100.24	99.73	101.14
Traces ppm									
Ba	474	195	105	216	178	301	193	145	425
Co	2	8	6	11	18	6	1	3	4
Cr	207	149	175	164	154	160	171	156	182
Cs	3.3	7.0	3.2	7.8	12.6	3.2	3.5	3.5	3.0
Ga	21.5	20.7	21.2	19.8	19.5	20.1	24.2	23.2	20.8
Hf	10.0	7.4	8.7	4.0	5.1	6.7	10.0	8.5	10.8
Nb	25.1	23.1	14.7	16.8	15.2	16.7	35.1	27.1	19.9
Ni	19	17	15	16	14	15	21	19	15
Rb	39	21	12	20	12	36	23	21	35
Sr	95	200	94	140	98	151	133	145	112
Ta	3.6	3.7	3.2	2.5	2.6	2.6	5.0	4.1	3.2
Th	47.5	50.2	41.2	18.4	13.9	29.0	46.7	50.0	35.2
V	10.3	22.3	22.1	37.8	41.4	18.1	11.1	18.1	14.6
Y	37.9	21.1	41.0	23.5	30.0	26.0	47.8	33.1	29.8
Zn	27	35	46	48	44	41	23	32	32
Zr	235	170	251	104	150	154	225	177	244
La	61.2	74.1	46.5	11.2	56.3	49.3	45.8	75.1	44.1
Ce	111.0	125.5	93.5	23.5	101.0	98.7	94.2	125.0	92.8
Pr	14.6	10.2	9.9	2.8	12.5	10.1	9.9	14.2	10.7
Nd	48.3	16.3	38.2	12.2	40.1	41.1	44.7	51.3	37.5
Sm	10.5	8.4	7.5	3.4	10.0	8.4	7.8	11.1	7.8
Eu	1.1	0.8	0.8	0.4	0.8	0.9	1.0	1.5	0.8
Gd	8.5	6.4	6.0	3.4	7.4	6.0	5.8	6.9	5.8
Tb	1.1	1.1	1.1	0.7	1.0	1.2	1.2	1.5	1.1
Dy	6.7	6.5	7.1	4.5	7.7	6.7	7.3	8.4	6.5
Ho	1.5	1.3	1.3	0.9	1.4	1.2	1.1	1.3	1.1
Er	4.7	4.2	4.2	3.2	5.2	5.1	5.8	6.2	5.2
Tm	0.9	0.7	0.8	0.5	0.8	0.7	0.4	0.9	0.7
Yb	4.4	4.1	3.8	3.2	5.3	3.5	4.0	5.5	3.7
Lu	0.7	0.5	0.6	0.6	0.6	0.8	0.8	0.9	0.6

Archive of SID

www.SID.ir

Petrographic evidences show that in Sargaz altered granites, Na-metasomatism occurred as sequentional events. As shown in Figure 8, the events begin with the formation of cracks in magmatic quartz grains (Fig. 8a) and then, very fine-grained new albite crystallizes in the cracks as crack-filling shape (Fig. 8b). Gradually, quartz grains dissolved more and more and a network of vugs produced. These vugs are filled by vug-filling albite shape (Fig. 8c). Dissolution of quartz grains and precipitation of new albite progressed, until just some parts of primary quartz grains survived as sporadic islands within large twinned new albite (interstitial albite) crystals (Fig. 8d). As Collins [12] stated, myrmekite forms by sudsolidus replacement processes in metasomatic granites. Collins and Collins [13] believe that Na- and Ca-metasomatism can produce myrmekite in granites just like Sargaz intrusion.

Na-metasomatism and other alteration processes caused some chemical changes in Sargaz granites. The altered rocks show Ca and K removal accompanied by Na-enrichment in relation to the least altered granites. The loss of Ca and K during Na-metasomatism has reported by Dall Agnoll [15] for hydrothermally altered granites from Amazonian craton. Some elements such as K, Mg, Ca, Fe and Co were depleted and the other ones such as Na,Yb, La, Nb, Al and Th enriched during metasomatism, while, Ti, Sc, Zr, Si and Zn acted as immobile elements (Figs. 9 and 10). The slightly increase of Al contents in altered samples (Table 2) is likely related to new albite formation simultaneously with the leaching of quartz similar those stated by Maruejol et al., [33], and Peterson and Eliasson, [39]. The depletion of Ca and Sr are likely related to the lack of crystallization of carbonates in the vugs and removal of these elements from environment [28].

Quartz Dissolution

Altered granites of Sargaz intrusion have been bleached and whitened during Na-metasomatism. Textural features indicate that the initial dissolution of magmatic cracked quartz grains accompanied by albitization of plagioclase and left a vugy reservoir rock, which facilitated fluid penetration and thereby further alteration and albite formation in the cracks and vugs. Alteration products of magmatic minerals imply that quartz dissolution occurred after emplacement and cooling of the host granite. In Sargaz granite, dissolution of quartz began along fractures which have been produced by Chah-Mazraeh fault movements. So, the fractures and cracks at the northern border of Sargaz intrusion may have caused Na-metasomatism, providing suitable pathways for fluids, dissolution of quartz and formation of new albite. Droschel and Rosenberg [19] reported a nonmagmatic fracture controlled hydrothermal system near Idaho batholith along a major brittle shear zone that produced an alteration assemblage of clays, chlorite, albite and quartz at an estimated temperature between 85-160 °C and 2.4-6.7 km depth.

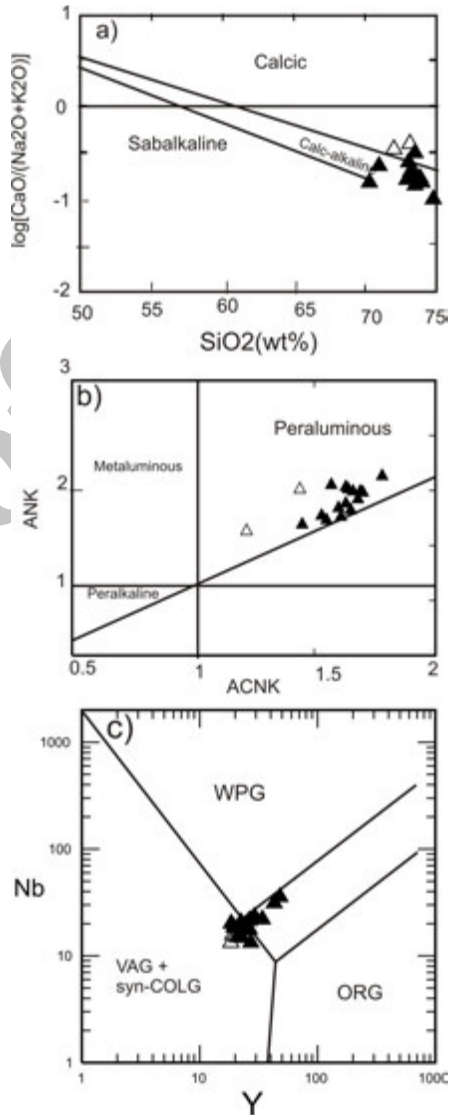

Figure 6. Composition of Sargaz granite in (a) the lime-alkali index diagram [9]; (b) ACNK versus ANK diagram [28]; (c) Y versus Nb diagram [33]. Abreviations in (c) denote ocean ridge granites (ORG), volcanic arc granites (VAG), within plate granites (WPG), and syn-collisional granites (syn-COLG). Open triangles: least altered Sagaz granites, black triangles: altered Sargaz granites.

www.SID.ir

As stated by Cathelineau [11], hydrothermal leaching of quartz from granite is frequently associated with sodium and/or potassium metasomatism, which alters the primary mineralogy, together with concomitant changes in the whole rock composition. This is characterized by chemically induced porosity enhancement due to the dissolution of magmatic quartz and subsequent replacement of the new albites in the cracks and microfractures of the Sargaz intrusion.

The Nature of Na-Metasomatism in Sargaz Intrusion

Na-metasomatism occurs just in the northern parts of the Sargaz intrusion resulting in a whitish color contrasting with the typical pinkish color of unaltered rocks in the central part of the intrusion. At first, fluid migration and Na-metasomatism developed along microfractures of quartz grains, suggesting that the process took place in an open system. Some authors ([11,39]) believe that albitization in granites usually follows the circulation of magmatic derived hydrothermal brines during postmagmatic and deutric events. In such process, albitization would be related to the internal structure of the crystalline massif, developing around the igneous massif and along tectonic lineaments. In Sargaz granite, the extent of Na-metasomatism is bonded to northern fracture zone, where the fluids have been migrated along the more permeable zones of the fractures.

Na-metasomatism is usually associated with albitization of K-feldspar or plagioclase which involves the coupled exchange reaction Na^{+} for Ca^{2+} and Si^{4+} for Al^{3+} [24]. Albite in granitic rocks may be formed by several processes; (1) magmatic crystallization; (2) exsolution of alkali feldspar, [40]; (3) de-anorthitization of plagioclase; (4) Na-metasomatic albitization [25,27]. In Sargaz intrusion, several lines of evidences show that new albite forming events are postmagmatic. In fact, overgrowth shapes of new albites (Fig. 3e) may have been formed by de-anorthitization process. This reaction involves a fluid phase, which introduces Na^{+} and Si^{4+} and releases Al^{3+} and Ca^{2+} from magmatic plagioclases according to the following reaction:

$Na_{0.8}Ca_{0.2}Al_{1.2}Si_{2.8}O_8$ (Oligoclase) + $0.2Na^{+}$ (aq) + $0.2H_2SiO_4$ (aq) = $NaAlSi_3O_8$ (Ab) + 0.2 Ca^{2+} (aq) + 0.2 Al^{3+} (aq) + 0.8 $(OH)^{-}$ (aq) (1) [25]

Putnis and Putnis [42] presented a coupled dissolution-reprecipitation mechanism in Na-metasomatic process that preserves the morphology and transfers crystallographic information from parent to product by epitaxial nucleation. Haapala [25] reported similar chessboard textures to those of albites formed in Sargaz granite (Figure 3a). In this process, primary

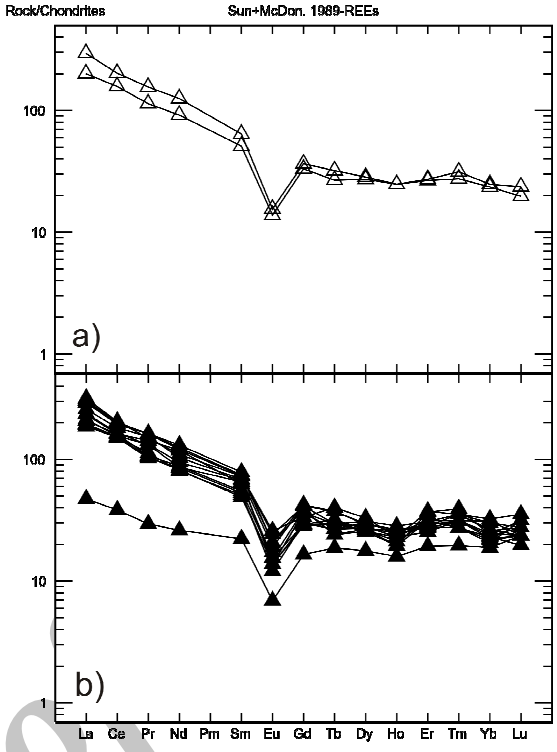

Figure 7. Chondrite-normalized Rare Earth elements (REE) Patterns of the least altered (a) and altered (b) rocks of Sargaz granites.

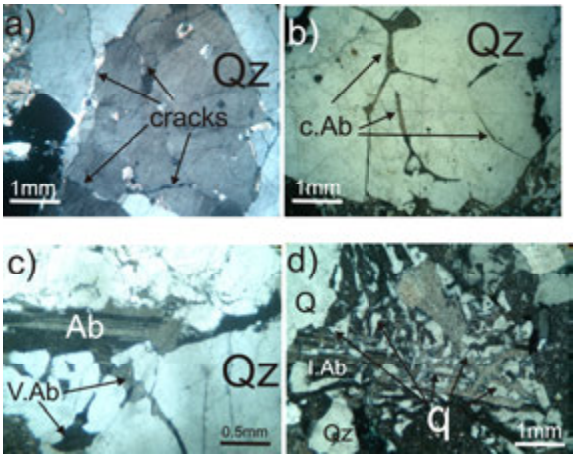

Figure 8. Textural features of sequentional stages of Na-metasomatism and formation of new albite in Sargaz altered granites; a) Formation of cracks on the magmatic quartz; b) Dissolution of quartz in the cracks and crystallization of albite in them (C.Ab); c) Progressive dissolution of quartz, formation of the vugs and precipitation of vug albite (V.Ab); d) Final stage of quartz dissolution and formation of interstitial albite (I.Ab). In this stage relics of magmatic quartz (q) survive as sporadic islands in the large new albite (Ab).

Archive of SID
www.SID.ir

plagioclases (oligoclases) have been altered into overgrowth and chessboard albites by the reaction (1) and dissolution- reprecipitation mechanism. Albites that form as crack-filling, vug-filling and interstitials need to fluid-rock interaction, dissolution of quartz and precipitation of albite from a fluid rather than coupled dissolution-reprecipitation mechanism. Dolejs and Wagner [18] performed a series of fluid/granite experiments and demonstrated that low temperature fluids (up to 400 °C) are richer in Na and Ca, and infiltration of these fluids into the granite produces Na-Ca metasomatism with aluminosilicate leaching and oxidation, whereas, high temperature fluids contain higher abundances of K and Fe and result K-Fe matasomatism. In Sargaz granitic intrusion, fluid has been a low temperature fluid activated the Na-metasomatism.

In experiments, the interaction of granites with low-temperature NaCl fluids produces Na enrichment, whereas, the hydrolytic alteration sequences by reaction with the high temperature fluid is distinctly potassic [18]. As shown in Figure 10, Na enrichment and K depletion has been occurred, thus low temperature NaCl brines have been reacted with the rocks. The brines were undersaturated in Si and invaded the microcracks of the quartz grains. The cracks in turn, acted as pathways for the fluid movement.

Mass balance studies in Sargaz granite during Na-metasomatism reveal that K, Rb, Fe, Mg, Ca, Sr, Co and Zn were depleted by breakdown of biotite and K-feldspar, while, Na was fixed in new albites. Petrographic aspects show that quartz has been dissolved in Sargaz altered granite during Na-metasomatism, but released Si has re-fixed in new albites. Thus in Figure 9 and 10, Si acts as immobile elements. During the formation of new albites in the cracks and vugs, Al was mobilized. Peralkaline fluids may probably facilitate the solubility and influx of Al to the system by Na-Al complexing [1]. Moreover, the presence of sericite inclusions in close association with albite indicate that Al^{3+} may be released from oligoclase as suggested by Leichman et al., [29]. Al^{3+} mobility during metasomatism has also been documented by Nijland and Touret [35].

Mechanisms of Fluid Infiltration

Na-metasomatism in the vicinity of fractures in the north of Sargaz granite indicates that the fractures played an important role in penetrating the fluids. Fracturing and microfracturing are well-established mechanisms for fluid infiltration in low-permeability rocks in both deep [3] and shallow crustal settings ([20,17,21,26]). Textures recorded in quartz grains (Figs. 3 and 5) in Sargaz granite emphasize the importance of fluid infiltration along microcracks as one way of providing fluid for mineral reaction. However, a part of fluid infiltration may be induced by an interface-coupled dissolution-reprecipitation mechanism.

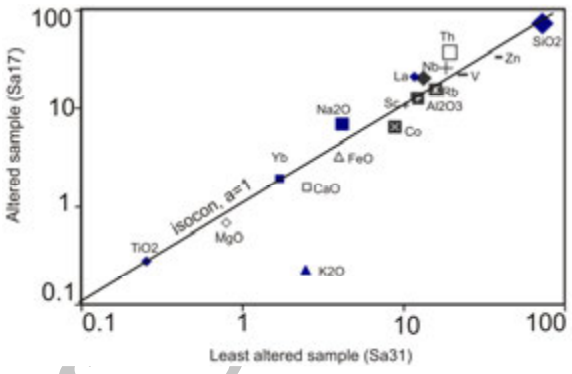

Figure 9. Log-log isocon diagram after Grant [20] for evaluating chemical changes during Na-metasomatism of Sargaz granites. An isocon with slope 1 is drawn and represents zero volume change. Major elements are plotted in wt%, trace elements in ppm.

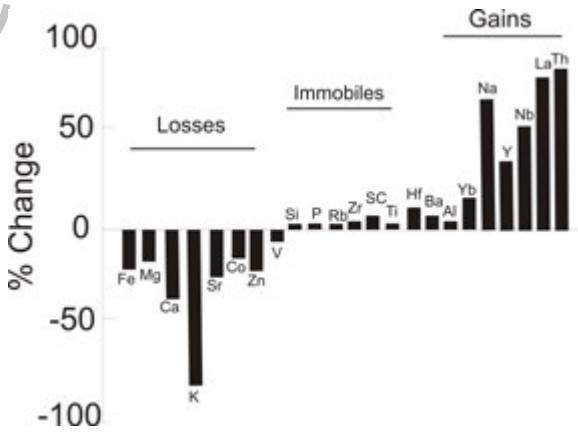

Figure 10. Diagram showing element losses, element gains and immobiles during Na-metasomatism in Sargaz granite.

Sources of Fluids

Two extreme types of fluids have been recorded as albitizing agents; (1) circulation of dilute aqueous fluids along a temperature gradient, close to chemical equilibrium with country rocks ([36,10]). An increase in temperature or pressure leads to an increase in the K/Na

Archive of SID

www.SID.ir

activity ratio in the equilibrium fluid phase and to maintain chemical equilibrium in the rock-fluid system, the rock must lose K and gain Na through exchange with the fluid. This exchange results in albitization of K-feldspars as follows ([36,10]):

$$KAlSi_3O_8 + (Na^+)_{aq} = NaAlSi_3O_8 + (K^+)_{aq} \quad (3)$$

(2) Highly saline fluids can also serve as albitizing agents, because sodium easily complexes with chlorine. This is particularly the case for albitization associated with some iron-rich oxide [5] and uranium deposits [30] or within mid-crustal shear zones [15]. High salinity of such albitizing fluids can be a primary magmatic feature [2] or be acquired either by interaction between aqueous metamorphic/magmatic fluids with evaporate rocks [5] or represents a primary characteristic of surface-derived brines [34]. Such brines can invade continental crust along faults within extentional setting [6]. Granite albitization can develop either during the hydrothermal activity associated with cooling of the intrusion [28] or long after this stage, totally disconnected with cooling [11]. Comparison of Na-metasomtism in Sargaz intrusion with well-defined similar cases, shows that low temperature NaCl brines could have been affected Sagaz granite. The above mentioned brines were probably surface-derived fluids that invaded the granite along Chah-Mazraeh related fractures and Na-metasomatic events occurred after cooling of Sargaz intrusion. The absence of chemical zoning in albites, suggests that the involved fluid did not undergo progressive changes in composition during Na-metasomatism.

Sequence of Na-Metasomatic Events in Sargaz Granite

The sequence of post magmatic events in Sargaz comprises:

1. The formation of fractures in northern part of Sargaz granitic intrusion and development of a dense system of closely spaced microcracks in magmatic quartz grains.
2. Infiltration and diffusion of alkali Na-rich fluids via the fractures.
3. Alteration of biotite into chlorite and hornblende into epidote, transformation of primary feldspars at their rims into chessboard albite and formation of overgrowth shapes of new albites.
4. Dissolution of magmatic quartz grains and formation of vugs. This process increased porosity which was sufficient for fluid circulation and promoted infiltration of Na-rich fluids and albite formation. In Sargaz intrusion, Na-metasomatism and quartz dissolution were closely linked and they may be considered as self-accelerated alteration process as suggested by Boulier and Charoy, [7]. Albitization of magmatic oligoclase (according to reaction (1)) in this stage, can release some Al required for the formation of new albites.
5. Precipitation of new albites in the cracks, vugs and the formation of interstitial albites. In this stage, most of new albites have been formed at the quartz grain boundaries. During the formation of these crystals, albite gradually grows into the adjacent quartz and eats the quartz (Fig. 3c and g).The undissolved parts of the quartz grains survive in contact with the new albite without changing their crystallographic orientations. The penetration of albite forming fluid into the quartz grains and dissolution of quartz began along microcracks of quartz and progressed until undissolved parts of the main quartz grains survived just as sporadic islands in the new albites (Fig. 5d). Sericitization process in Sargaz intrusion occurred in this stage.
6. Silicification and formation of quartz veinlets.

All evidences show that in northern part of the Sargaz granitic intrusion, a network of closely packed fractures developed by Chah-Mazraeh fault and this process promoted fluid circulation and caused a distinct Na-metasomatism in this part. This metasomatism is characterized by the formation of new albite, quartz dissolution, propylitization and some chemical and textural changes in the original granite. Different forms of albites such as overgrowth, crack-filling, vug-filling and interstitial albites have been formed in this metasomatic event. These evidences and Na-metasomatism can be mentioned in the Iranian granitic intrusions as a basis for the gold and uranium exploration studies.

Acknowledgments

The authors would like to thank Shahid Bahonar University of Kerman for financial support. The authors also thank to professor A. Aftabi for helpful discussion and aid with the English revision. We thank Dr. Jasper Bernth for performing electron microprobe analyses in Carlslohe University.

References

1. Anderson K.I., Burnham C.W. Feldspar and the transport of aluminum under metamorphic conditions. American Journal of Sciences, **283**A, 283– 97 (1983).
2. Aslund T., Oliver N.H.S., Cartwright I. Metasomatism of the Revenue Granite and aureole rocks, Mt Isa Inlier, Queensland: syndeformational fluid flow and fluid–rock

Archive of SID

www.SID.ir

interaction. Australian Journal of Earth Sciences **42**, 291–299 (1995).
3. Austrheim H. Eclogitization of lower crustal granulites by fluid migration through shear zones. Earth and Planetary Science Letters **81**, 221-232 (1987)
4. Babakhani A., Sabzehei M., Alavi Tehrani N. and Valeh N. Geological quadrangle map of Iran, No. J12, scale: 1:250000, Geological Suvey of Iran (1992).
5. Barton M.K., Johnson D.A. Evaporitic-source model for igneous-related Fe oxide-(REE–Cu–Au–U) mineralization. Geology, **24**, 259–262 (1996).
6. Battles D.A., Barton M.D. (1994) Arc-related sodic hydrothermal alteration in the western United States. Geology, **23**, 913–916 (1994).
7. Boullier A.M. and Charoy B. Fluctuation in porosity and fluid pressure during hydrothermal events: textural evidence in the Emuford District, Australia. Journal of Structural Geology, **16**(10),1417-1429 (1994).
8. Boulvais P., Rufet G., Cornichet J., Mermet M. Cretaceous albitization and dequartzification of Hercynian peraluminous granite in the Salvezines Massif (French Pyrenees). Lithos, **93** ,89-106 (2007).
9. Brown G.C. Calc-alkaline intrusive rocks: their diversity, evolution, and relation to volcanic arcs. In: Thorpe, R.S. (Ed.), Andesites, Orogenic andesites and Related Rocks. Wiley, Chichester, pp. 437-461 (1982).
10. Carten R.B. Sodium–calcium metasomatism: chemical, temporal, and spatial relationships at the Yerington, Nevada, porphyry copper deposit. Economic Geology, **81**, 1495–1519 (1986).
11. Cathelineau M. The hydrothermal alkali metasomatism effects on granitic rocks: Quartz dissolution and related subsolidus changes, Journal of Petrology, **27** (4), 945-965 (1986).
12. Collins L.G. Origin of myrmekiteand metasomatic granite: Myrmekite, ISSN 1526-5757, electronic internet publication, no. 1, (1996)
13. Collins L.G. and Collins B.J. Myrmekite formation at Temecula, California, revisited: A photomicrographic essay illustrating replacement textures: Myrmekite, ISSN 1526-5757, electronic internet publication, no. 43 (2002)
14. Coutinho, M.G., Liverton, T., Souza, E.C. Granitic magmatism and related gold mineralization on the Tapajo´s Mineral Province, Amazonian Area, Brazil. 2nd Int. Symp. Gran. Ass. Miner. Salvador, Brazil Abstr. Progr., pp. 46-47 (1997).
15. Dall'Agnol R. Etudes sur des granites du type 'Rondonian'en Amazonie Orientale et leurs transformations tardimagmatiques. Doctorate Thesis, University of Paul Sabatier, Tolouse, France (1980).
16. De Jong G., Williams P.J. Giant metasomatism system formed during exhumation of mid-crustal Proterozoic rocks in the vicinity of the Cloncurry Fault, northwest Queensland. Australian Journal of Earth Sciences **42**, 281–290 (1995).
17. Dipple G.M., Ferry J.M. Metasomatism and fluid flow in ductile fault zones, Contribution to Mineralogy and Prtology, **112**, 149-164 (1992).
18. Dolejs D. and Wagner T. Thermodynamic modeling of non-ideal mineral-fluid equilibria in the System Si-Al-Fe-Mg-Ca-Na-K-H-O-Cl at elevated temperatures and pressures: Implications for hydrothermal mass transfer in granitic rocks, Geochemica et Cosmochemica Acta, **72**, 526-553 (2008).
19. Druschel G.K., Rosenberg P.E. Non-magmatic fracture – controlled hydrothermal systems in the Idaho Batholith: South Fork Payette geothermal system, Chemical Geology, **173**, 271-291 (2001).
20. Engvik A. K., Bertram A., Kalthoff J. F., Stockhert B., Austrheim H. & Elvevold S. Magma-driven hydraulic fracturing and infiltration of fluids into the damaged host rock, an example from Dronning Maud Land, Antarctica. Journal of Structural Geology **27**, 839-854 (2005).
21. Fitz Gerald J. D. & Stunitz H. Deformation of granitoids at low metamorphic grade. 1. Reactions and grain-size reduction. Tectonophysics **221**, 269-297 (1993).
22. Ghergari L., Maris C. Petrology and geochemistry of the Mare granitoid (Northern Apuseni Mountains), Romania, tudia Universitatis Bebes-Bolyai, Geologia, **52**(2), 11-18 (2007).
23. Goldfarb, R.J., Groves, D.I., Gardoll, S. Orogenic gold and geologic time: a global synthesis. Ore Geology Reviews, **19**, 1-75. (2001).
24. Grant J.A. The Isocon Diagram — a ssimple solution to Gresens' equation for metasomatic alteration. Economic Geology, **81**, 1976–1982 (1986).
25. Haapala I. Magmatic and post magmatic processes in tin-mineralized granites: Topaz-bearing leucogranite in the Eurajoki rapakivi granite stock, Finland, Journal of Petrology, **38**(12), 1645-1659 (1997).
26. Jamtveit B., Putnis C. V. & Malthe-Sorenssen A. Reaction induced fracturing. Contributions to Mineralogy and Petrology **157**, 127-133 (2009).
27. Juliani C., Correa-Silva R.H., Monteiro L.V.S., Bettencourt J.S., Nunes C.M.D. The Batalha Au granite system- Tapajos Gold Province, Amazonian craton, Brazil: hydrothermal alterationand regional implication, Precambrian Research, **119**, 225-256 (2002).
28. Lee M.R. and Parsons I. Dislocation formation and albitization in alkali feldspars from the Shap granite, American Mineralogist, **82**, 557-570 (1997).
29. Leichmann J., Broska I. & Zachovalova K. Low-grade metamorphic alteration of feldspar minerals: a CL study. Terra Nova **15**, 104-108 (2003).
30. Lobato L.M., Fyfe W. Metamorphism, metasomatism and mineralization at Lagoa Real, Bahia, Brazil. Economic Geology, **85**, 968–989 (1990).
31. Maghraoui M.El., Joron J.L., Raimbault L. and Treuil M. Element mobility during metasomatism of granitic rocks in the Saint-Chely d'Apcher area (Lozere, France), Environmental International, **28**, 349-357 (2002).
32. Maniar P.D., Piccoli P.M. Tectonic discrimination of granitoids. Geol. Soc. Am. Bull. **101** (5), 635- 643 1989.
33. Maruéjol P., Cuney M., Turpin L. Magmatic and hydrothermal REE fractionation in the Xihuashan granites (SE China). Contributions to Mineralogy and Petrology, **104**, 668–680 (1990).
34. McLelland J., Morrison J., Selleck B., Cunningham B., Olson C., Schmidt K. Hydrothermal alteration of late- to post-tectonic Lyon Mountain Granitic Gneiss, AdirondackMountains, New York: Origin of quartz–sillimanite segregations, quartz–albite lithologies, and

Archive of SID

www.SID.ir

associated Kiruna-type low-Ti Fe-oxide deposits. Journal of metamorphic Geology, **20**, 175–190 (2002).
35. Nijland T. G. & Touret J. L. R. Replacement of graphic pegmatite by graphic albite-actinolite-clinopyroxene intergrowths (Mjavatn, southern Norway). European Journal of Mineralogy, **13**, 41-50 (2001).
36. Pascal M.L. Les albitites du massif de l'Agly (Pyrénées Orientales). Ph.D. thesis, Ecole Nationale Supérieure des Mines, Paris, France, 163 pp (1979).
37. Pearce J.A., Harris N.B., Tindle A.C. Trace elements discrimination diagrams for the tectonic interpretation of granitic rocks. Journal of Petrology **25**, 56- 983 (1984).
38. Perez R.J. and Boles J.R. An empirically derived kinetic model for albitization of detrital plagioclase, American Journal of Science, **305**,312-343 (2005).
39. Petersson J. and Eliasson T. Mineral evolution and element mobility during episyenitization (dequartzfication) and albitization in the postkinematic Bohus granite, southwest Sweden, Lithos, **42** (1-2), 123-146 (1997).
40. Plumper O. and Putnis A. The complex hydrothermal history of granitic rocks: multiple feldspar replacement reactions under subsolidus conditions, Journal of petrology, **50** (5), 967-987 (2009).
41. Putnis A., Hinrichs R., Putnis C. V., Golla-chindler U. & Collins L. G. Hematite in porous red-clouded feldspars: Evidence of large-scale crustal fluid=rock interaction. Lithos, **95**, 10-18 (2007a).
42. Putnis A. and Putnis C.V. The mechanism of reequilibriation of solid in the presence of a fluid phase, Journal of Solid State Chemistry, **180**, 1783-1786 (2007).
43. Rubenach M.J. and Lewthwaite K.A. Metasomatic albitites and related biotite-rich schists from a low-pressure polymetamorphic terrane, Snake Creek Anticline, Mount Isa Inlier, north-eastern Australia: microstructures and P-T paths, Journal of Metamorphic Geology, **20**, 191-202 (2002).
44. Yuguchi T. and Nishiyama T. The mechanism of myrmekite formation deduced from steady-diffusion modeling based on petrography: case study of the Okueyama granitic body, Kyushu, Japan, Lithos, **106**, 237-260 (2008).

Archive of SID

www.SID.ir